A radiometric airborne geophysical survey of the Isle of Wight

David Beamish and James C. White

British Geological Survey, Keyworth, Nottingham, NG12 5GG, UK.

Published in PGA, Special Issue, November 2011

Proceedings of the Geologists' Association 122 (2011) 787–799

Corresponding author:

David Beamish (dbe@bgs.ac.uk)

British Geological Survey, Keyworth, Nottingham NG12 5GG, UK

Tel: +44(0) 115 936 3432

Fax: +44(0) 115 936 3437

Email: dbe@bgs.ac.uk

Keywords: airborne geophysics, gamma-ray, radiometric, Isle of Wight, bedrock geology, GIS

Right running head:

Airborne radiometric survey IoW

ABSTRACT

A high resolution airborne geophysical survey across the Isle of Wight and Lymington area conducted in 2008 provided the first modern radiometric survey across the geological formations that characterise much of southern England. The basic radiometric data is presented and it is evident that bedrock geology exerts a controlling influence on the broad response characteristics of the naturally-occurring radioelements. A GIS-based geological classification of the data provides a quantitative assessment and reveals that a relatively high percentage of the variability of the data is explained by the Cretaceous bedrock geology but this is much reduced in the Palaeogene. The three traditional Chalk units (Lower, Middle and Upper Chalk depicted on the currently available Geological Map) provide the lowest and most distinct behaviour within the Cretaceous sequence. Mineral content within the Chalk appears to decrease with increasing age. A new method of representing the baseline radiometric information from the survey in terms of the mean values of the geological classification is presented. The variation of radioelement geochemistry within individual formations is examined in two case studies from the Cretaceous Lower Greensand Group and the Palaeogene Hamstead Member (Bouldnor Formation). The Cretaceous sequences provide the higher levels of discrimination of localised variations in radioelement distributions. A more detailed case study examines the potential influences from the degree of water saturation in the soil and superficial deposits.

1. Introduction

A number of modern, high-resolution, multi-parameter geophysical surveys have been conducted over the past decade across onshore UK (Figure 1). These High Resolution Airborne Resource and Environmental (HiRES) surveys have acquired radiometric (gamma-ray spectroscopy), magnetic and electromagnetic (conductivity) measurements at 200 m line spacings and at low altitude (< 60 m). The earliest survey (HiRES-1) across the north Midlands (Figure 1) used a lower survey resolution of 400 m and a typical flight altitude of ~ 90 m. The present study considers the small radiometric data set acquired over the Isle of Wight (IoW) and part of the Lymington area (Figure 1) in 2008.

Airborne radiometric data are acquired over a wide gamma-ray energy spectrum and the spectral data are routinely processed to provide estimates of the naturally occurring abundances of the radiogenic materials potassium, thorium and uranium. The main component of gamma-ray flux is typically contained within the upper 30 cm of the Earth's surface. The airborne measurements thus provide a geochemical mapping capability obtained from concentrations of these materials in the upper 0.5 m.

The distribution of radioelements in rocks and soils is discussed by Dickson and Scott (1997) and is further reviewed by IAEA (2003). Potassium is a major component of the Earth's crust (2.35%). It is an alkali element and shows a simple chemistry. The major hosts of potassium in rocks are potassic feldspars (e.g. orthoclase microcline with ~13%) and micas (e.g. biotite and muscovite with 8%). Thorium is a minor component of the Earth's crust (~12 ppm). Major thorium bearing minerals (e.g. monazite and zircon) are stable during weathering and may accumulate in heavy mineral sand deposits. Thorium freed by the breakdown of minerals during weathering may be retained in Fe or Ti oxides/hydroxides and with clays. Uranium is a reactive metal with a low average abundance in the Earth's crust (~ 3 ppm). It may be present in rocks as the oxide and silicate minerals, uraninite and uranothorite; as

trace amounts in other minerals or along grain boundaries possibly as uranium oxides or silicates.

Gamma ray surveys are used in several fields of science. They are used for geological, geochemical, and environmental mapping, and allow the interpretation of regional features over large areas (IAEA, 1991, 2003). They may be used to estimate and assess the terrestrial radiation dose to the human population and to identify areas of potential natural radiation hazard. Regional surveys also provide a baseline data set against which man-made contamination can be estimated. The existing UK HiRES radiometric data sets have been applied to a range of such geoscience investigations many of which have focussed on environmental, health and soil science issues. An airborne and ground-based radiometric study considered the use of such data in relation to its potential to assess indoor radon levels (Scheib et al., 2006). The close correlation between airborne uranium measurements and indoor radon concentrations has been further developed using other HiRES data sets (Appleton et al., 2008).

A combination of HiRES-1 data and trial survey data were used to assess radioelement concentrations associated with coal-mine waste (Emery et al., 2005) that included ground follow-up studies. Lahti et al. (2001) and Lahti and Jones (2003) describe the distribution of man-made radioactive sources located by HiRES surveys, including colliery spoil heaps, iron ore mines and processing centres, fly ash adjacent to coal-fired power station sites, Chernobyl fallout (i.e. the man-made radionuclide Caesium, ^{137} Cs), nuclear reprocessing plant discharges and an isolated ^{60}Co source. Scheib and Beamish (2010) report the distribution of ^{137}Cs (largely Chernobyl-derived) across the northern UK based on the HiRES survey data.

The airborne datasets can also provide detailed information about the characteristics of the soil and its parent geological material, including surface texture, weathering, leaching, soil depth, moisture and clay mineralogy (Bierwirth, 1997). The degree to which the HiRES radiometric data can be used to provide thematic maps of soils, particularly soil texture, in Eastern England was considered by Rawlins et al. (2007). The overall correlations of airborne radiometric estimates with soil survey data for potassium and thorium were large indicating that the two radioelements provide effective estimates of their concentrations in the soil and their distribution patterns.

Parent material accounted for significant amounts of the observed variability. The study confirmed that the HiRES radiometric components potassium and thorium provide information on parent material and associated geochemistry in the 'young' landscapes of England and Wales.

In the UK context, the HiRES IoW survey, and the three geophysical data sets acquired in the south of England are highly distinct. Systematic airborne geophysical survey measurements in the south of England are confined to a vintage data set acquired as part the Mineral Reconnaissance Programme between 1957 and 1959 across south-west England (Cornwell et al., 1995). By modern standards, the radiometric information obtained was crude. Baseline geochemical sampling (e.g. (Johnson et al., 2005) is also absent for much of the south of England, so there is no pre-existing geochemical context for the airborne measurements The Palaeogene and Cretaceous bedrock formations encountered on the IoW (Figure 2) are some of the youngest lithologies to be assessed by the HiRES surveys. Since the lithologies are also representative of much of the southern mainland of England, the geochemical information afforded by the radiometric survey is significant.

The distribution of soil types on the IoW is considered to reflect the underlying solid and superficial geology (Entec, 2008). The superficial deposits are relatively sparse and thin and although assessments of the radiometric data can be undertaken using such data, we confine ourselves here to an assessment of information relating to bedrock geology. The bedrock geology is considered here to be the parent material for the overlying soils.

A Geographical Information System (GIS) based approach has been adopted in order to arrive at an assessment of the baseline data (e.g. the statistical means for each of the formations) together with their variations across individual formations. These latter investigations relate to the geochemical variability within formations. In these young formations, the variability encountered will largely relate to the sedimentation/deposition process itself together with any subsequent weathering and erosion.

2 Survey: Location and details

The Isle of Wight is England's largest island; situated off the south coast of Hampshire (Figure 1) it offers a diverse range of geology for an area of its size (380 km^2). During September and October 2008 the island was surveyed in 10 flying days as part of the High Resolution Airborne Resource and Environment Surveys (HiRES) program. The survey logistics and further details are provided by Beamish and Cuss (2009). The primary aim of the survey was to determine the geophysical responses of the specific geology, characteristic of much of southern England, in relation to current geological map revision. The survey obtained over 4,500 line km of data and effectively provided the first modern airborne radiometric survey undertaken across southern England.

The full survey area covered a total on- and off-shore rectangular area of 36 x 22 km (792 km^2) which was investigated with flight lines spaced at 200 m and flown in an N-S direction, orthogonal to the major structural trends of the region. A nominal survey altitude of 56 m was adopted but over the built environment a regulatory flight altitude of 240 m was required. In forming the survey rectangle, a small area on the mainland (Lymington area) was included to provide continuity of information. The sampling of the radiometric data (see later) provided 74,441 survey measurements.

The geology of the Isle of Wight can be fairly evenly divided into a northern zone of Palaeogene sands, clays and limestones and a southern region of Cretaceous strata. The structure is dominated by a prominent east-west trending monoclonal fold or ramp structure (White, 1921; Melville and Freshney, 1982). The two zones are divided by the east-west trending chalk beds of the late-Cretaceous (Figure 2). The youngest units on the island are the Oligocene succession of the Cranmore Member and Hamstead Member (HM-CLSS, Figure 2) of the Bouldnor Formation.

The main component of the present study comprises an assessment of the radiometric data in relation to the current 1:50 000 scale digital data for bedrock geology: DiGMap-GB50 version 5.18, BGS (2008). The 22 bedrock units, together with the

rock lexicon codes used here are shown in Figure 2. The map also shows polygons (in cross-hatch) that identify the major urban areas and a series of contours (in red) within which the survey altitude was greater than 100 m. The central vertically elongate ellipse is due to the avoidance of a major mast, and this zone forms a small hole in an otherwise uniform data set.

It is worth remarking that the complete survey rectangle contains a large extent of seawater. The magnetic component (see White and Beamish, 2010, *this issue*) of the survey is unaffected by water bodies however the radiometric response from such bodies is theoretically zero. When only onshore radiometric data are assessed, the number of available measurements (IoW and mainland) is reduced to 34,973. The IoW onshore survey comprises 31,578 radiometric measurements. Additionally, the spatial extent of bedrock outcrop on the IoW is often limited because of the high dip of the strata, particularly across the east to west monoclinal spine of the island. Across this area, outcrop zones may possess widths of only 50 m or less. Within such narrow zones, the radiometric sampling may locally reduce to 1 measurement point only along a flight line.

3 The radiometric data

The geophysical data includes airborne 256-channel gamma spectrometry covering the energy range from 0.3-3 MeV. The radiometric data are sampled at 1 second intervals which, for this survey, equates to a travelling distance of approximately 60 m over the ground. A range of corrections are applied to the data including removing aircraft, cosmic and radon background; application of stripping corrections derived from calibration data and application of height attenuation corrections. These are based on protocols described in IAEA (1991) and by Grasty and Minty (1995a,b). The geophysical calibration and processing of the IoW survey data is described in detail by White et al. (2009).

The fully corrected count rate data are used to estimate the concentrations in the ground of each of the three radioelements, potassium, uranium and thorium. The procedure determines the concentrations that would give the observed count rates, if uniformly distributed in an infinite horizontal slab source. Because the uranium and thorium windows actually measure ^{214}Bi and ^{208}Tl , respectively, the calculation

implicitly assumes radioactive equilibrium in the uranium and thorium decay series. The uranium and thorium concentrations are therefore expressed as equivalent concentrations, eU and eTh, in ppm. Potassium (^{40}K) is processed to produce equivalent ground concentrations in %K. Total counts are here converted into cps (counts per second). A dose rate can also be estimated, using full spectral techniques or by calculating from the concentrations of K%, eU (ppm) and eTh (ppm).

3.1 Radiometric Assessments

Gamma ray spectroscopy measures radioelement concentrations to a depth of about 0.5 m (IAEA, 2003). In exposed rock the main component of the radiation may be detected from first 30 cm although this depth will increase for lower density unconsolidated materials. In dry peat the main measured component of radiation may extend to several metres. A uniform distribution of the radionuclides is assumed in the data conversions. In general this is probably a reasonable assumption, but it will not hold true in all circumstances. Because of this potential non-uniformity, radionuclide concentrations should be regarded only as estimates of actual ground values. They are, in any case, an average of the ground activities within the field of view, or 'footprint' of the airborne gamma spectrometer.

The ground area or 'footprint' from which most of the contribution of radioactivity to each one second measurement has the form of an ellipse elongated in the flight direction. For example, at 56 m altitude, 75% of the measured radiation will come from a width of about 150 m, extending to around 220 m along the flight line (Pitkin and Duval, 1980), although this varies with source geometry characteristics (Billings et al., 2003; Grasty et al., 1979). Within that ellipse, the greatest contribution will, in general, come from directly beneath the aircraft and will fall off exponentially with lateral distance from the flight line. At the increased survey height over urban areas, the field of view would be considerably larger.

Varying levels of soil moisture may influence the airborne radiometric measurements (IAEA, 2003). Clays with specific radium content tend to register a higher eU level when wet whereas sandy soils can register a lower eU when wet (Grasty, 1997). The

IoW survey was carried out during good weather conditions (no rain) and so temporal washout and variable soil moisture should not be an issue in the interpretation. In general there is a well established correlation between gamma-ray attenuation and soil moisture (Carroll, 1981). Typically a 10% increase in soil moisture content will reduce the radiation flux at the surface by about the same amount (Grasty, 1997).

3.2 Survey Results

The radiometric data are first summarised in terms of colour images obtained from minimum-curvature grids. Bodies of water produce a null (theoretically zero) radiometric response. In order to avoid image colour bias, the radiometric images have been cut to the coast. Figure 3a shows the radiometric data in terms of Total Count which is a measure of total radioactivity over the spectrum from 0.3 to 3 MeV. The image shown uses an equal-area normalisation of the colour scale. The data indicate the composite radiogenic activity of the formations. It is evident that there is a significant geological control of the radiometric responses observed. The central chalk units are identified as having very low responses. This is not surprising given their remarkable purity with an estimated content of between 90% and 98% calcium carbonate. Even with their low response values, spatial variations are detected. The Wealden Group from the early Cretaceous in the SW of the island clearly displays a locally high concentration response. Persistently high values are also observed throughout the majority of the Palaeogene in the north.

The contributions from the 3 radioelements potassium, uranium and thorium are summarised in the Ternary image of Figure 3b. The Ternary image is a normalised (to an equal-area histogram) 3–way colour stretching of the contributions from the individual radioelements with red representing potassium, blue representing uranium and green representing thorium. The presentation is standard method in radiometric processing and interpretation (IAEA, 2003). In areas where all three radioelement concentrations are low, the Ternary image shows black; when all three concentrations are high, the Ternary response tends to white. The limiting behaviour (i.e. the 3-element highs and lows) in the Ternary image is also reflected in the high and low zones within the Total Count image of Figure 3a. The Ternary image, while

containing more noise, is able to reveal more subtle features in the relative radioelement contributions. In terms of equivalent radiometric concentrations the response is dominated by thorium (Table 1). In detail particularly strong and diagnostic potassium signatures are found in the Cretaceous Upper Greensand and Gault formations and are likely to be generated by higher abundances of clay minerals. The Lower Greensand Group Ferruginous Sands Formation, partially because of its large area, reveals a spatially complex set of radiometric signatures with a strong thorium response evident across some significant areas of the formation. A major portion of the Palaeogene in the north is dominated by higher amplitudes in all three radioelements. Interestingly the Ternary character of the western-most Headon Beds (Headon Hill Formation) observed on the island (with a significant uranium response) appears to be distinct from that observed on the mainland (with a higher potassium contribution).

The individual radioelement statistics of the data sets summarised in Figure 3 (i.e. onshore data values only and with high altitude survey data included) are given in Table 1. The original data set of 74,411 values is reduced to 34,973 in this onshore assessment. The statistical distributions of the data are discussed later.

Table 1

Summary statistics of the onshore radiometric data set (N=34,973), including the IoW and the Lymington area covered by the survey.

Radioelement	Minimum	Maximum	Mean	Std. Dev.
Total Count (cps)	-0.27	10.43	4.98	1.45
Thorium (eTh, ppm)	-0.57	12.62	4.71	1.85
Uranium (eU, ppm)	-1.32	4.72	1.11	0.60
Potassium (%K)	-0.14	2.11	0.79	0.29

It is evident from the images presented and on further inspection in relation to geological line-work that the radiometric data display a high degree of correlation with bedrock geology. This is explored further in the analysis described below.

4 Geological Classification of the radiometric data

One of the purposes of this study is to summarise the radiometric responses in terms of the young geological bedrock formations found on the IoW. Superficial deposits are not extensive on the IoW but can be included in an equivalent assessment. Appleton (2009) conducted a detailed GIS-based analysis of the application of the radiometric data in relation to geological mapping of both superficial deposits and bedrock geology. The methodology used here is a simplified version of that GIS-based analysis approach.

The 1:50 000 scale digital data for bedrock geology BGS (2008) based on surveys conducted prior to the current survey) is shown in Figure 2. The 22 bedrock units, and their lexicon codes are described in Table 2. The geological polygons, acting as parent materials in the assessment, were then attributed with the radiometric data. The procedure enables a statistical assessment of the radiometric data according to geological classification.

Table 2

Bedrock geological classification for the Isle of Wight

LEX_ROCK	BEDROCK NAME	BEDROCK LITHOLOGY
HM-CLSS	HAMSTEAD BEDS	CLAY, SILT AND SAND
BMBG-CAMU	BEMBRIDGE MARLS	CALCAREOUS MUD
BMBG-CLAY	BEMBRIDGE MARLS	CLAY

BEL-LMAR	BEMBRIDGE LIMESTONE FM.	LIMESTONE AND [SUBEQUAL/SUBORDINATE] ARGILLACEOUS ROCKS, INTERBEDDED
HE-CLSS	HEADON FM.	CLAY, SILT AND SAND
HEOS-CLSS	HEADON BEDS AND OSBORNE BEDS (UNDIFFERENTIATED)	CLAY, SILT AND SAND
HEOS-LMST	HEADON BEDS AND OSBORNE BEDS (UNDIFFERENTIATED)	LIMESTONE
BRBA-CLSS	BRACKLESHAM GROUP AND BARTON GROUP (UNDIFFERENTIATED)	CLAY, SILT AND SAND
LC-CLSS	LONDON CLAY FM.	CLAY, SILT AND SAND
LMBE-CLSS	LAMBETH GROUP (READING FM.)	CLAY, SILT AND SAND
LPCK-CHLK	LEWES NODULAR CHALK FM., SEAFORD CHALK FM., NEWHAVEN CHALK FM., CULVER CHALK FM., PORTSDOWN CHALK FM. (WHITE CHALK)	CHALK
WNPCK-CHLK	WEST MELBURY MARLY CHALK FM., ZIG ZAG CHALK FM., HOLYWELL NODULAR CHALK FM. AND NEW PIT CHALK FM.	CHALK
WZCK-CHLK	WEST MELBURY MARLY CHALK FM. AND ZIG ZAG	CHALK

	CHALK FM. (UNDIFFERENTIATED) (GREY CHALK)	
UGS-SDST	UPPER GREENSAND FM.	SANDSTONE
UGS-SDCH	UPPER GREENSAND FM.	SANDSTONE AND CHERT
GLT-MDST	GAULT FM.	MUDSTONE
CAW-SDSM	CARSTONE (ISLE OF WIGHT)	SANDSTONE, SILTSTONE AND MUDSTONE
SIOW-SDSM	SANDROCK FM.	SANDSTONE, SILTSTONE AND MUDSTONE
FRS-FGST	FERRUGINOUS SANDS FM.	FERRUGINOUS SANDSTONE
AC-MDST	ATHERFIELD CLAY FM.	MUDSTONE
W-MDST	WEALDEN GROUP	MUDSTONE
W-SDST	WEALDEN GROUP	SANDSTONE

It may be useful to condition (e.g. exclude) portions of airborne geophysical data prior to conducting a statistical geological appraisal. Data exclusion for offshore locations has already been noted. Geological polygons also exclude major inland water bodies so no further conditioning with regard to null (non-geological) data values is usually required.

The airborne radiometric data may be less reliable in urban areas because a significant proportion of the ground area is covered in buildings and/or asphalt paving, and the flight altitude is approximately 240 m compared with about 56 m over rural areas. Negative uranium (eU) values tend to characterise urban areas (Appleton et al., 2008) although they also occur in areas where eU is near the detection limit and the removal

of background results in negative values. Appleton (2009) conducted a statistical analysis of the radiometric data within the large (>1 km^2) urban areas (e.g. Figure 2) and 500-m wide buffer zones around the urban areas, with data grouped by bedrock geology. The results indicate that the averages for urban areas are 87% to 89% of those in the surrounding rural area.

In the following analysis the data set has first been restricted to locations where the survey altitude is less than 100 m. This condition also has the equivalent effect of restricting the data set over urban areas (see Figure 2). The radiometric data were then directly attributed with the 1:50,000 scale bedrock geology polygons. The resulting number of samples in each bedrock class is listed in Table 3 along with two central moment statistics of the classified radiometric data. An examination of the statistical distributions obtained by geological classification indicates that no one simple model (e.g. normal or log-normal distributions) can be assumed across the range of results of the assessment. In a number of cases, bimodal distributions are observed. In these circumstances we quote both the arithmetic and geometric means of the populations in Table 3. The nature of the individual distributions is further illustrated in the box-whisker plots discussed below.

The Digital Terrain Model (DTM) obtained by the airborne survey, and referred to geoid (WGS-84) height, is also listed. The Headon Formation (HE-CLSS) provides values at only 6 locations (across two outcrop zones) and this is too small to be considered statistically representative. This formation aside, the analysis provides population statistics that vary between 22 samples (HEOS-LMST) and 6330 samples (HM-CLSS).

Table 3

Arithmetic and geometric means of the radiometric-bedrock classification analysis. TC refers to Total Count. The first number of each radiometric column (TC, %K, eU and eTh) is the arithmetic mean and the second number is the geometric mean of the observed distribution.

LEX_ROCK	No. data	DTM (m)	TC (cps)	% K	eU (ppm)	eTh (ppm)
HM-CLSS	6330	80.6	6.22, 5.90	0.96, 0.92	1.32, 1.19	5.87, 5.61
BMBG-CAMU	2027	69.7	5.49, 5.12	0.90, 0.83	1.20, 1.05	5.26, 4.83
BMBG-CLAY	1362	67.5	5.73, 5.35	0.91, 0.84	1.27, 1.12	5.49, 5.01
BEL-LMAR	829	83.02	4.44, 3.42	0.71, 0.56	1.10, 0.90	4.02, 3.57
HE-CLSS	6	80.97	7.83, 7.73	1.25, 1.28	1.82, 1.52	7.64, 7.46
HEOS-CLSS	1716	66.93	3.93, 2.98	0.64, 0.48	0.91, 0.74	3.62, 2.83
HEOS-LMST	22	98.9	4.33, 4.26	0.67, 0.65	1.08, 1.02	3.98, 3.94
BRBA-CLSS	1034	88.9	5.03, 4.93	0.81, 0.77	1.16, 1.03	4.59, 4.40
LC-CLSS	256	107.3	4.98, 4.92	0.82, 0.79	1.13, 1.02	4.49, 4.32
LMBE-CLSS	198	112.9	4.36, 4.23	0.68, 0.64	0.95, 0.82	3.94, 3.70
LPCK-CHLK	2278	161.7	3.00, 2.82	0.37, 0.32	0.68, 0.57	2.88, 2.45
WNCK-CHLK	960	141.2	3.29, 3.13	0.49, 0.43	0.66, 0.54	2.95, 2.64
WZCK-CHLK	796	221.0	4.09, 3.94	0.65, 0.58	0.81, 0.67	3.94, 3.65
UGS-SDST	1368	150.2	5.27, 5.15	0.94, 0.91	1.25, 1.08	4.34, 4.11
UGS-SDCH	120	175.6	4.87, 4.80	0.88, 0.86	1.12, 0.98	3.86, 3.61
GLT-MDST	1150	127.9	5.10, 5.00	0.95, 0.91	1.11, 0.98	4.23, 3.97
CAW-SDSM	730	119.1	5.49, 5.37	0.89, 0.85	1.18, 1.04	5.53, 5.27
SIOW-SDSM	1434	110.9	4.62, 4.49	0.75, 0.70	1.04, 0.91	4.29, 4.02
FRS-FGST	5098	88.80	5.26, 5.11	0.79, 0.75	1.15, 1.00	5.30, 5.00
AC-MDST	277	81.30	5.79, 5.66	0.82, 0.78	1.46, 1.32	5.64, 5.40

W-MDST	976	71.6	6.28, 5.89	0.87, 0.80	1.55, 1.38	6.32, 5.76
W-SDST	32	75.3	5.70, 5.41	0.85, 0.81	1.44, 1.28	5.18, 4.78

The results of Table 3 indicate that a general assumption that the data are normally distributed (arithmetic mean) will tend to provide higher 'average' estimates than if the data are assumed to be log-normally distributed (geometric mean). It is also evident from Table 3 that the lowest radiometric mean responses are associated with the Chalk units and the highest responses are associated with the Cretaceous Wealden Formation (W-MDST).

The geological classification of the data is shown graphically in the box-whisker plot of Figure 4. The analysis provides one such plot for each of the four radiometric components. Figures 4a,b show the Total Count and potassium results and Figures 4c,d show the thorium and uranium behaviour, respectively. For each individual unit, the infilled box indicates the first and third quartiles of the distribution with the enclosed cross-bar denoting the median value. The terminating bars denote the range of the data and the discrete symbols indicate outliers.

Perhaps the most distinct behaviour is the response of the Upper Chalk (LPCK-CHLK) which provides the lowest radiometric response in all channels. The three chalk units also display significantly lower responses then the older Wealden Clays, Greensand and Gault units of the Cretaceous sequence. As indicated in Figure 4, there is a progressive decrease in Total Count and potassium up the Chalk sequence (Figure 4a,b). The progression is less evident in the thorium and uranium responses (Figure 4c,d). The behaviour suggests a decreasing mineral content (e.g. clay) with decreasing age. The non-Chalk sequences of the Cretaceous tend to show a level of response overlap although the Total Count shows some ability to provide a level of discrimination across units.

The Wealden Group mudstone and sandstone (W-MDST and W-SDST) display the largest radiogenic response (i.e. Total Count) within the Cretaceous although the sample of W-SDST comprises only 32 samples. Discounting the small statistical

sample of the Headon Beds (HE-CLSS), the analysis of the Palaeogene sequence indicates that the three youngest units (Hamstead Beds, HM-CLSS, the Bembridge Marls, BMBG-CLAY and BMBG-CAMU) provide a larger radiometric response than the six older units.

4.1 ANOVA analysis

The information on the ability of the radiometric measurements to discriminate geological bedrock units can be further analysed, in fact summarised, using an analysis of variance (ANOVA). The ANOVA model analysis operates by comparing the amounts of dispersion in each of the groups to the total amount of dispersion in the data. The ANOVA analysis tests the hypothesis that the means of two or more of the populations are equal. The ANOVA results shown in Table 4 summarise the proportion (as a percentage) of the radiometric data set that can be explained by the geological classification. The geological classifications used were the Cretaceous units, the Palaeogene units and across all geological units (e.g. Table 3).

Table 4

Results of ANOVA analysis. Percentage of variability explained by bedrock geology

	Cretaceous	Palaeogene	All geological units
Total Count (cps)	43 %	21 %	35 %
potassium (%K)	40 %	18 %	31 %
thorium (eTh)	34 %	18 %	29 %
uranium (eU)	17 %	5 %	13 %

The proportion of the variability explained is relatively high for the Cretaceous units and significantly lower for the Palaeogene succession. As Table 4 indicates, the behaviour across all geological units then falls between the results obtained for the

two subdivisions. Total Count provides the greatest discrimination and uranium the least. Whilst the results presented thus far can be potentially used to guide geological remapping (e.g. Appleton, 2009), the variability (heterolithic nature of many of the geological units) within individual units is sufficiently large to make this a challenging task. The most informative results provided by the survey data are, in fact, the variability, and the scales of variability, within the formations. This additional new information is discussed later.

4.2 Baseline radiometric maps

The geological classification of the radiometric data provided statistical means that can be used to generate new baseline radiometric maps for the IoW. Such maps also provide a summary of the analysis conducted. The conditioned data set used in the analysis contains gaps and holes due to the altitude condition applied. These omitted zones are now populated with their associated bedrock mean values. We here use the geometric means listed in Table 3. Figure 5 shows two examples of the new baseline radiometric maps produced. Figure 5a shows the Total Count information which can be considered a summary of the radiogenic behaviour of the Cretaceous and Palaeogene formations located on the IoW. The image uses an equal-area colour scale. Figure 5b shows the radiometric Ternary baseline map obtained for the IoW. The majority of the formations can be seen to have distinctive radioelement responses. A strong potassium (pink) response from the Upper Greensand (UGS-SDST) formation is preseded by the stronger (red) response of the Gault Clay (GLT-MDST). A distinctive light green (thorium) response is associated with the older Carstone Formation (CAW-SDSM) (Monk's Bay Sandstone Formation herein, Hopson et al., *XXXX, this issue*) and the adjacent Sandrock Formation (SIOW-SDSM) displays a darker green (thorium) response. Perhaps the most interesting feature of this map is the response of the Atherfield Clay Formation (AC-MDST) which shows a distinctive uranium (blue) response along with the adjacent Wealden Group Formation (W-MDST). Both of these distinctive responses are far less evident in the high variability information content of the conventional Ternary display (Figure 3b).

It is also worth recording the gamma-ray exposure/dose levels obtained from the survey data. The ground-level distribution of dose rate will follow that of the Total Count data shown in Figures 3 and 5. The ground-level dose rates calculated for the data have a mean of 29 nGy/h with maximum of 46 nGy/h (nanogray per hour). These are among the lowest levels of exposure/dose rates recorded by the HiRES surveys, as we would expect given the nature of the geological formations. By way of reference, the typical dose rate due to background cosmic rays, at sea level, is about 32 nGy/h (IAEA, 2003).

5 Inter formation variations

Both the gridded data sets (Figure 3) and the box-whisker plots (Figure 4) provide some information on the variations of the radiometric data within and across the geological units encountered on the IoW. A more detailed examination of the behaviour proceeds by assessing the spatial variations within the 22 geological units. Various methodologies have been considered in relation to summarising the radiometric behaviour observed. The sequence of results shown in Figure 6 provides an indication of the procedures. As noted previously a significant number of the IoW formations exist as thin and elongate outcrops, particularly in association with the central spinal structure. The summaries presented here use the formations with the largest spatial extent. We first use the Lower Greensand Ferruginous Sand Formation as an example from the Cretaceous succession followed by the Hamstead Member as an example of the Palaeogene (Oligocene) succession.

5.1 Lower Greensand Formation

Figure 6 shows the results obtained across the Lower Greensand Ferruginous Sand Formation. (FRS-FGST). The FRS-FGST succession broadly comprises a number of coarsening-upwards units, dark grey sandy muds passing up into fine to medium, grey-green glauconitic sands. There are reported to be five cycles of sedimentation in

the FR-FGST, each going from glauconitic clay (possibly with a high %K and eTh radiometric signature) to clean sands (possibly with a lower %K and eTh signature).

Figure 6a shows the outcrop polygon containing a 1:250k topographic location map. To the east of the map, the urban conurbation of Shanklin-Sandown is identified by a polygon with infill. Figure 6b shows a gridded image of the Total Count data restricted to the polygon. The image colour scale uses an equal-area colour-scale distribution and the dynamic range is increased over that using the complete data set (e.g. Figure 3). In order to examine the behaviour of the data away from the mean value, a number of statistical techniques may be employed (e.g. by examining the distribution of the upper and lower quartiles). Figure 6c shows the results of a cluster analysis of the Total Count data. Cluster analysis is the assignment of a set of observations into subsets (clusters) so that observations in the same cluster are similar in some sense. The method and algorithm used here is described in the ESRI ArcMap™ Geoprocessing Toolbox. The method provides scores (called z and p values) that measure the statistical significance of the analysis and indicate whether the apparent similarity (or dissimilarity) in values for a feature and its neighbours is greater than one would expect from a random distribution. The results shown in Figure 6c show the clusters with the highest z-scores (>2.58) that trace both high and low amplitude features in the data. When these results are compared with the gridded data image in Figure 6b, it is apparent that there is a broad level of correspondence with a few notable exceptions (identified within ellipses). Both sets of information reveal that there exist significant localised radiometric response signatures at a variety of scales.

The next stage in summarising the radiometric data for geological/geochemical application is to combine the three radioelement components in a Ternary colour image. Once again, in using data confined to a single formation, the dynamic range is increased over that in the complete data set (Figure 3b). The image obtained, although subject to noise from all three components (particularly the low amplitude eU response) provides a highly diagnostic assessment of the radioelement variations across the formation. In the east, the northern area shows a dominant thorium response with some strong edges (arrowed). Moving south, a dispersed uranium

response is evident that is bordered in the west (in the vicinity of Godshill) by a significant potassium response. Moving west, a change in character is observed across an N-S arcuate zone (arrowed). Further west, thorium dominates a considerable portion of the WNW striking limb. There are also notable dark (low amplitudes in all components) zones across the Ternary image. At the scale shown, these display an apparent association with the river systems of the eastern Yar and the Medina towards the centre of the image (see Figure 6a). The landform and low radiometric response associations with the river system and potential saturated ground are examined in greater detail later across the more detailed 5 x 5 km rectangle shown in Figure 6a.

5. 2 Hampstead Formation

As can be seen in the whole survey Ternary image of Figure 3b, the Palaeogene provides a response that is generally distinct from the older formations. Persistent white zones indicate high values in all three radiometric components. This is actually the result of a high degree of correlation between potassium and thorium within the Palaeogene units while uranium is of low amplitude and spatially variable. The coefficient of linear correlation (R^2) between potassium and thorium for the Hamstead Member is 36% which compares with only 13% for the Lower Greensand formation considered previously.

The Hamstead Member (HM-CLSS) consists of coloured clays, loams, sands and shales deposited in a brackish freshwater environment (White, 1921). A third marine stage is recorded in some of the uppermost beds (Melville and Freshney, 1982). We would anticipate that the highest radiometric amplitudes to be associated with clay rich parent materials. Figure 7a shows the HM-CLSS polygon containing a 1:250k topographic location map. The area contains portions of the largest urban centres on the island Cowes in the north and Newport in the south). Figure 7b shows a gridded image of the Total Count data restricted to the polygon and survey elevations of less than 100 m. The image colour scale uses an equal-area distribution and the dynamic range is increased over that using the complete data set (e.g. Figure 3). Maximum ranges in Total Count are in fact similar to those of the Lower Greensand.

The three radioelement components are combined into a Ternary colour image in Figure 7c. The image obtained, is subject to noise in all three components; particularly that of the low amplitude eU response. Due to the high potassium-thorium correlation, radioelement discrimination of features is more difficult than in the Cretaceous formations. Using both Total Count and the Ternary image a few zones may be defined as partially distinct. In the east, a broad change in character is observed across a zone that is delineated by the dash lines. The eastern-most section shows a degree of diffuse banding in the NNE-SSW direction. The centre of the formation, in the vicinity of the conurbations, displays fairly rapid response variations from high to low values. Further west and outlined by the ellipse is a zone of more constant character in the Ternary response. Finally, a strip along the coastal zone (arrowed) is defined by equal amplitude potassium and thorium responses with only minor contribution from uranium.

5.3 Lower Greensand Formation (detail)

As noted previously, there is an indication that low response values across the formation show some associations with river systems. The response obtained from the water body itself will be theoretically zero, however the lateral scale of the river systems considered here (e.g. the Eastern Yar) is relatively narrow. In relation to the field of view of the airborne sensor the influence of the water body on each measurement should be minimal. A second question then arises as to whether there is a further attenuating contribution from the degree of water saturation within the river catchment. There is a well established spatial correlation between gamma-ray attenuation and soil moisture (Caroll, 1981). As noted previously, a 10% increase in soil water leads to a reduction in gamma radiation by about the same amount (Grasty, 1997). The 5 x 5 km study area, largely confined to the Lower Greensand (indicated in Figure 6a) was chosen to further understand the response to soil moisture. Figure 8a shows the selected area with the relief provided by an accurate 5 x 5 m resolution DTM. A map of the superficial deposits (those deposits currently shown within BGS (2008)) has been overlaid on the grey coloured DTM. Alluvium (clay, silt, sand and gravel) is coloured yellow, river terrace deposits (sand and gravel) are coloured

orange and peat deposits are shown in brown. Contour values of the lowest values of Total Count are shown in blue (transparent) on the same topographic background in Figure 8b. Values defined by the blue contours range from 1.5 to 4.5 cps. The upper limit represents the lower quartile of the Total Count distribution across the 5 x 5 km area that provides 2028 measurements. The actual river system may be better discerned in map form in Figure 8c. In Figure 8b, four main zones of low count are labelled A, B, C and D. Zones A and C would connect using a slightly higher threshold than the upper limit shown. The three zones labelled A, B and C show a high degree of correspondence with the course of the river Eastern Yar and associated alluvial deposits. In the south of the area, zones A and B contain areas of peat deposits. The two zones are separated by higher ground. The low Total Count associations are not altogether simple. The prominent oxbow feature does not feature in the low contour distribution and a significant zone of low values (zone D) is associated with high ground above the incised river valley in the west.

The observations, although requiring much further study, have two main implications. The first is that the radiometric responses may be subject, in detail, to influences from water saturation in the soil and superficial deposits. The observation is somewhat surprising since the local soils are generally regarded as free draining (see below). Secondly, the low values of Total Count, and potentially the associated individual radiometric contributions, may provide information on the degree of local saturation in the near-surface. The majority of the IoW Lower Greensand groundwater body is typically covered by free-draining argillic brown earth soils (Soil Survey, 1983). In a recent review of the water body, Entec (2008) noted the occurrence of stagnogleyic brown earth soils, characterised as having a slowly permeable subsoil. The study notes small areas of clayey, gley soils along the Eastern Yar downstream of (i.e. to the north) of Godshill and on a short stretch of the upper Medina west of Godshill (to the west of the study rectangle). The soil type often indicates areas where the ground is often waterlogged due to a shallow groundwater table.

To complete our analysis of the study area, the map of superficial deposits is replaced by an Ordnance Survey 1:50k topographic map in Figure 8c. The Eastern Yar river system, including tributaries, can be noted in blue. The upper quartiles of the individual radiometric are shown as coloured contours with potassium in red, thorium in Green and uranium in blue. The quartile values used are 0.96 (%K), 6.50 (eTh,

ppm) and 1.50 (eU, ppm). It is evident that the major contributions occur (and may be limited by) to the north and west of the river valley of the Eastern Yar, The study area largely comprises the Lower Greensand and it is likely that the river valley marks a significant change in character in geochemistry of the formation. On the rising ground to the north, there is dominant zone of thorium while towards the centre a large zone of potassium tends to prevail. In the SW corner a zone enriched in all three radioelements is apparent.

6. Conclusions

The study has reviewed the information content of the first modern radiometric survey in the south of England. The IoW survey is significant in assessing the radiometric response of the Palaeogene and Cretaceous formations common to much of southern England. The processed geophysical data has been presented across the IoW and across the mainland Lymington area in terms of Total Count and the three radioelements potassium, thorium and uranium. The Palaeogene formations on the mainland appear to be distinct from those on the IoW in terms of the differing contributions from the three radioelements (e.g. Ternary image of Figure 3b). There is an apparent high degree of bedrock geological control on the radiometric responses that has been further investigated and quantified using GIS-based procedures.

The results of the survey have been analysed according to the existing bedrock classification at a scale of 1:50,000 and assuming the bedrock acts as parent material for the near-surface radiogenic concentrations. The results provide stable means and population statistics over 21 of the 22 bedrock formations encountered. The most distinct behaviour is that of the Upper Chalk which provides the lowest radiometric response in all elements. The three chalk units display lower responses then the older Wealden Clays, Greensand and Gault units. There is a progressive decrease in Total Count and potassium up through the Chalk sequence (Figure 4). The progression is less evident in the thorium and uranium responses. The behaviour suggests a decreasing mineral content (e.g. clay) with decreasing age. The non-Chalk sequences of the Cretaceous tend to show a level of response overlap. The results across the Palaeogene sequence indicate that the youngest units (Hamstead Member and the

Bembridge Marls Member) provide a larger radiometric response than the older six units. We have proposed a new method of presenting the baseline radiometric information from the survey in terms of the 'mean' values of each geological classification. Given the complete statistical descriptions of the geologically classified data (e.g. Figure 4), the mean values of the statistical populations represent significant reference estimates that can ultimately be used for the prediction of radiometric properties elsewhere in the UK. The information provided (Figure 5) is thus a useful geological-radiometric statistical summary of the behaviour of each formation. The data means used are inherently low noise and we believe the combined Ternary baseline image reveals some distinctive and precise formation attributes that would, otherwise, have gone undetected.

The degree of data variability that can be explained by geological classification was investigated using an analysis of variance (ANOVA). Potassium provides the greatest discrimination and uranium the least. The proportion of explained variability is significantly higher (typically double) for the Cretaceous than the Palaeogene. The ANOVA results indicate significant variability within the majority of formations. These variations relate to subtle changes in geochemical attributes that can be detected even across the main outcrop of the Upper Chalk (Figure 3). We have presented case studies across two of the larger areas within the Cretaceous and Palaeogene sequences. Due to the relatively high correlation of potassium and thorium within the Palaeogene, discrimination of localised features is more readily achieved in the Cretaceous formations. Low response values displaying some associations with river systems (the Eastern Yar) were investigated in greater detail. It appears that the radiometric responses may be subject, locally, to influences from water saturation in the soil and superficial deposits. These observations together with much of the detailed information provided by the survey will require further study.

Acknowledgement

Our thanks go to Cathy Scheib and Peter Hopson for internal reviews and helpful comments. Topographic base maps are reproduced from the OS by British Geological Survey with the permission of Ordnance Survey on behalf of the Controller of Her

Majesty's Stationery Office, Crown copyright. All rights reserved. A newscast of the Isle of Wight airborne geophysical survey is available on the BGS YouTube channel at http://www.youtube.com/watch?v=D4ECcUPNi_E , last accessed 01 September 2010.This paper is published with the permission of the Executive Director, British Geological Survey (NERC).

References

Appleton, J. D., 2009. Application of HiRES airborne radiometric data for geological mapping of the Isle of Wight. British Geological Survey Internal Report IR/09/015.

Appleton, J.D., Miles, J.C.H., Green, B.M.R, Larmour, R., 2008. Pilot study of the application of Tellus airborne radiometric and soil geochemical data for radon mapping. Journal of Environmental Radioactivity 99, 1687–1697.

Beamish, D., Cuss, R.J., 2009. The HiRES airborne geophysical survey of the Isle of Wight: Logistics Report. *British Geological Survey Internal Report* IR/09/54.

Bierwirth, P.N., 1997. The use of airborne gamma-emission data for detecting soil properties. *Proceedings of the Third International Airborne Remote Sensing Conference and Exhibition.* Copenhagen, Denmark.

Billings, S., Minty, B.R., Newsam, G.N., 2003. Deconvolution and spatial resolution of airborne gamma-ray surveys. Geophysics 68, 1257-1266.

British Geological Survey, 2008. Digital Geological Map of Great Britain 1:50 000 scale (DiGMapGB-50) data. Version 5.18. Keyworth, Nottingham: British Geological Survey. Tiles EW330_Lymington; EW331_ Portsmouth; EW344_Chale; EW345_Ventnor. Release date 30-09-2008.

Carroll, T. R., 1981. Airborne moisture measurements using natural terrestrial gamma radiation. Soil Science 132, 358-366.

Cornwell, J.D., Kimbell, S.F., Evans, A.D., Cooper, D.C., 1995. A review of detailed airborne geophysical surveys in Great Britain, *Mineral Reconaissance Programme Report*, British Geological Survey, No. 136.

Dickson, B.L., Scott, K.M., 1997. Interpretation of ariel ganmma-ray surveys – adding the geochemical factors. AGSO Journal of Australian Geology and Geophysics 17, 187-200.

Emery, C., Davis, J.R., Hodgkinson, E., Jones, D.G., 2005. Airborne and ground-based radiometric investigation of colliery spoil near Shirebrook, the English Midlands. *British Geological Survey Internal Report* IR/05/59.

Entec UK limited, 2008. Environment Agency – Southern region, Groundwater Body Groundwater Quality Reports, Isle of Wight Lower Greensand Body Final Report,1-106.

Grasty, R.L., 1997. Radon emanation and soil moisture effects on airborne gamma ray measurements. Geophysics 62, 1379-1385.

Grasty, R.L., Kosanke, K.L., Foote, R.S., 1979. Fields of view of airborne gamma-ray

detectors. Geophysics 44, 1447-1457

Grasty, R.L., Minty, B.R.S., 1995a. A guide to the technical specifications for airborne gamma-ray surveys. Australian Geological Survey Organisation, Record, 1995/20.

Grasty, R.L., Minty, B.R.S., 1995b. The standardisation of airborne gamma-ray surveys in Australia. Exploration Geophysics 26, 276-283.

Hopson, P.M., Wilkinson, I.P., Woods, M.A., Farrant, A.R., *XXXX*. The Monk's Bay Sandstone Formation (formerly the Carstone of the Isle of Wight), its distribution, litho- and biostratigraphy. Proceedinghs of the Geologists' Association, *this issue.*

IAEA, 1991. Airborne gamma ray spectrometer surveying, International Atomic Energy Agency, Technical Report Series, No. 323.

IAEA, 2003. Guidelines for radioelement mapping using gamma ray spectrometry, International Atomic Energy Agency, Technical Report Series, No. 1363.

Johnson, C.C., Breward, N., Ander, E.L., Ault, L., 2005. G-BASE: baseline geochemical mapping of Great Britain and Northern Ireland. Geochemistry: Exploration, Environment, Analysis 5, 347-357.

Lahti, M., Jones, D.G., Multala, J, Rainey, M.P., 2001. Environmental applications of airborne radiometric surveys. Expanded Abstracts, 63rd Annual Conference, European Association of Geoscientists and Engineers.

Lahti, M., Jones, D.G., 2003. Environmental applications of airborne radiometric surveys. First Break 21. 35-41.

Melville, R.V., Freshney, E.C., 1982. British Regional Geology: Hampshire Basin and adjoining areas (Keyworth, Nottingham: British Geological Survey).

Pitkin, J.A., Duval, J.S., 1980. Design parameters for aerial gamma-ray surveys. Geophysics 45, 1427-1439.

Rawlins, B.G., Lark, R.M., Webster, R., 2007. Understanding airborne radiometric survey signals across part of eastern England. Earth Surface Process and Landforms 32, 1503-1515.

Scheib, C., Appleton, J.D., Jones, D., Hodgkinson, E., 2006. Airborne gamma spectrometry, soil geochemistry and permeability index data in support of radon potential mapping in Central England. In: Barnet, I., Neznal, M., Pacherova, P. (Eds.), Proceedings of the 8th International Workshop on the Geological Aspect of Radon Risk Mapping, 26–30 September 2006, Prague, Czech Republic. Czech Geological Survey, RADON Corp., Prague, 210–219.

Scheib, C., Beamish, D., 2010. High spatial resolution observations of ^{137}Cs in northern Britain and Ireland from airborne geophysical survey. Journal of Environmental Radioactivity 101, 670-680.

Soil Survey of England and Wales, 1983. 1:250 000 Soil Map, Sheet 6, South East England.

White, H.J.O., 1921. A short account of the geology of the Isle of Wight. British Geological Survey Memoir.

White, J.C, Beamish, D., Cuss, R.J., 2009. The HiRES airborne geophysical survey of the Isle of Wight: Processing Report. British Geological Survey Open Report OR/09/060.

White, J.C, Beamish, D., *XXXX*. Magnetic structural information obtained from the HiRES airborne survey of the Isle of Wight. Proceedinghs of the Geologists' Association, *this issue.*

Figure Captions

Figure 1. Location map of main UK HiRES airborne geophysical surveys. The Isle of Wight survey is identified in the south.

Figure 2. The 1:50 000 scale digital data for the bedrock geology (DiGMap-GB50 version 5.18) of the Isle of Wight, BGS (2008). The red contours denote areas where the survey altitude was greater than 100 m. The polygons with cross-hatch in black denote urban areas. The geological code key is further described in Table 2.

Figure 3. Radiometric images obtained from the gridded data across the complete survey area but omitting bodies of water. (a) Total Count and (b) Ternary colour plot of the relative contributions made by the %K, eTh and eU components of the data set.

Figure 4. Box and whisker plots summarising the statistical behaviour of the radiometric data classified according to bedrock geology (a) Total Count. (b) Potassium (%K). (c) Thorium (eTh) and (d) Uranium (eU). A trend, with age, across the 3 Chalk units is indicated. The geological key codes are further defined in Figure 2 and in Table 2.

Figure 5. Average (mean) baseline radiometric response of the 22 bedrock formations obtained by statistical analysis (a) Total Count and (b) Ternary colour image.

Figure 6. Summary of the radiometric information for the Cretaceous Lower Greensand Group Ferruginous Sand Formation (FRS-FGST). (a) Outcrop polygon containing 1:250k OS topographic map and a 5 x 5 km location rectangle of a detailed

study area. (b) Gridded image of the Total Count data. (c) Results of cluster analysis of the Total Count data. (d) Ternary colour image.

Figure 7. Summary of radiometric information for the Palaeogene Hamstead Member (HM-CLSS). (a) Outcrop polygon containing 1:250k OS topographic location map. (b) Gridded image of the Total count data. (c) Ternary colour image.

Figure 8. Summary of radiometric information across a detailed 5 x 5 km area mainly within the Lower Greensand (see Figure 6a). Perspective views looking north. (a) Map of superficial deposits overlaid on a grey DTM. Alluvium (clay, silt, sand and gravel) is coloured yellow, river terrace deposits (sand and gravel) are coloured orange and peat deposits are shown in brown. (b) Contours of lowest values (< 4.5 cps) of Total Count shown as blue contour regions (transparent) overlaid on a grey DTM. (c) OS 1:50,000 base topographic map overlaid on a DTM with contoured areas of high (third quartile) values of Potassium (red), Thorium (green) and Uranium (blue).


Ayr
Northern Ireland
(Tellus)
Anglesey
North Midlands
Isle of Wight

Figure 1

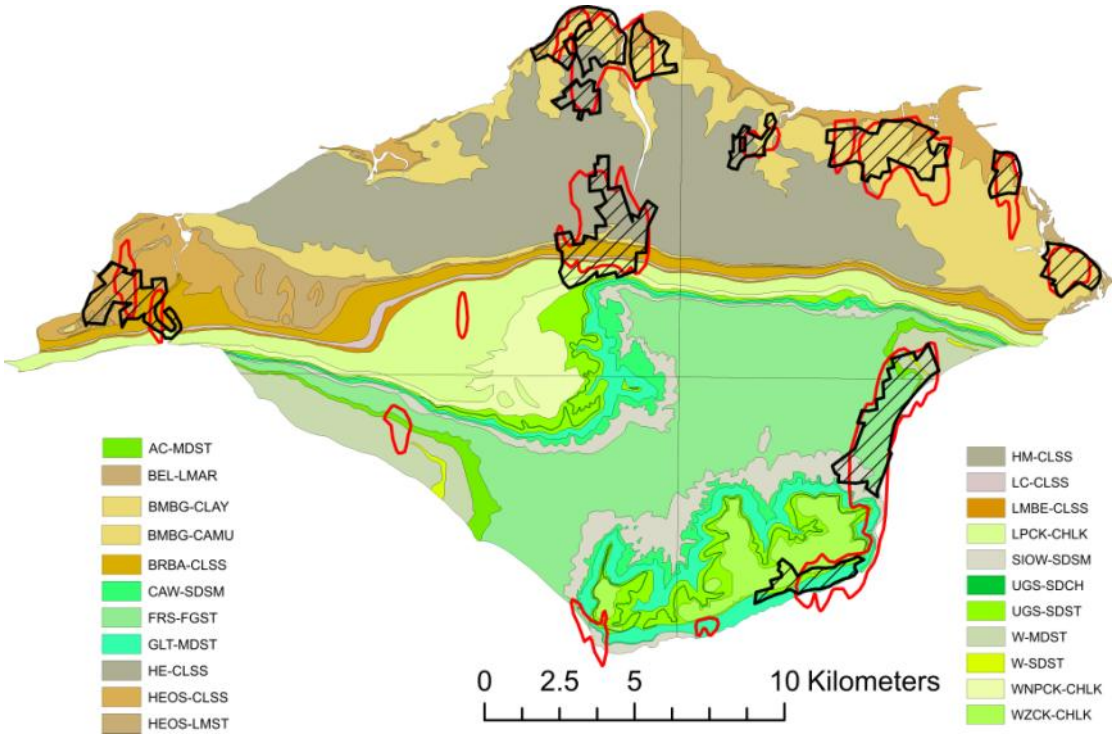
AC-MDST
BEL-LMAR
BMBG-CLAY
BMBG-CAMU
BRBA-CLSS
CAW-SDSM
FRS-FGST
GLT-MDST
HE-CLSS
HEOS-CLSS
HEOS-LMST
HM-CLSS
LC-CLSS
LMBE-CLSS
LPCK-CHLK
SIOW-SDSM
UGS-SDCH
UGS-SDST
W-MDST
W-SDST
WNPCK-CHLK
WZCK-CHLK
0 2.5 5 10 Kilometers

Figure 2

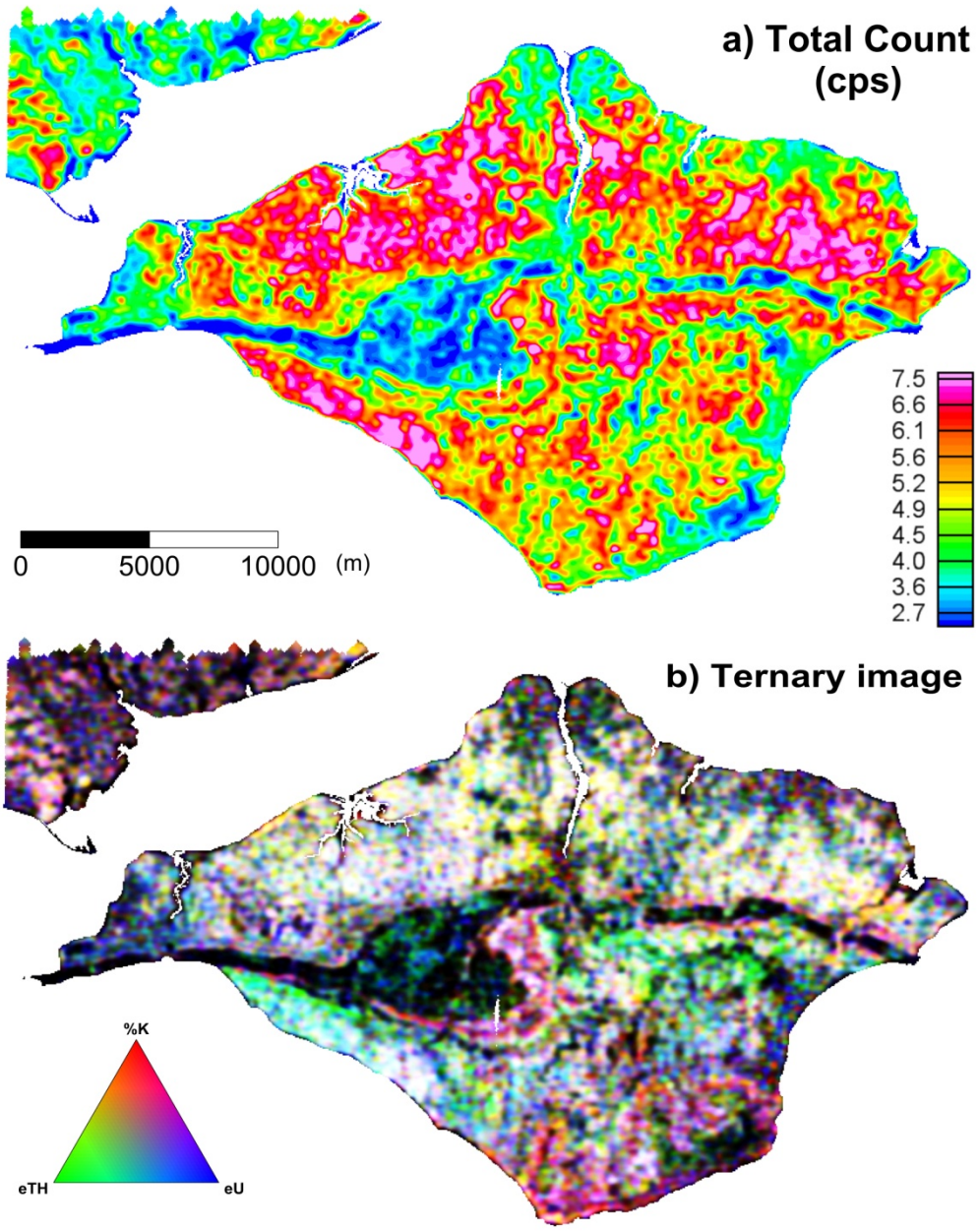
a) Total Count
(cps)
7.5
6.6
6.1
5.6
5.2
4.9
4.5
4.0
3.6
2.7
0
5000
10000
(m)
b) Ternary image
%K
eTH
eU

Figure 3

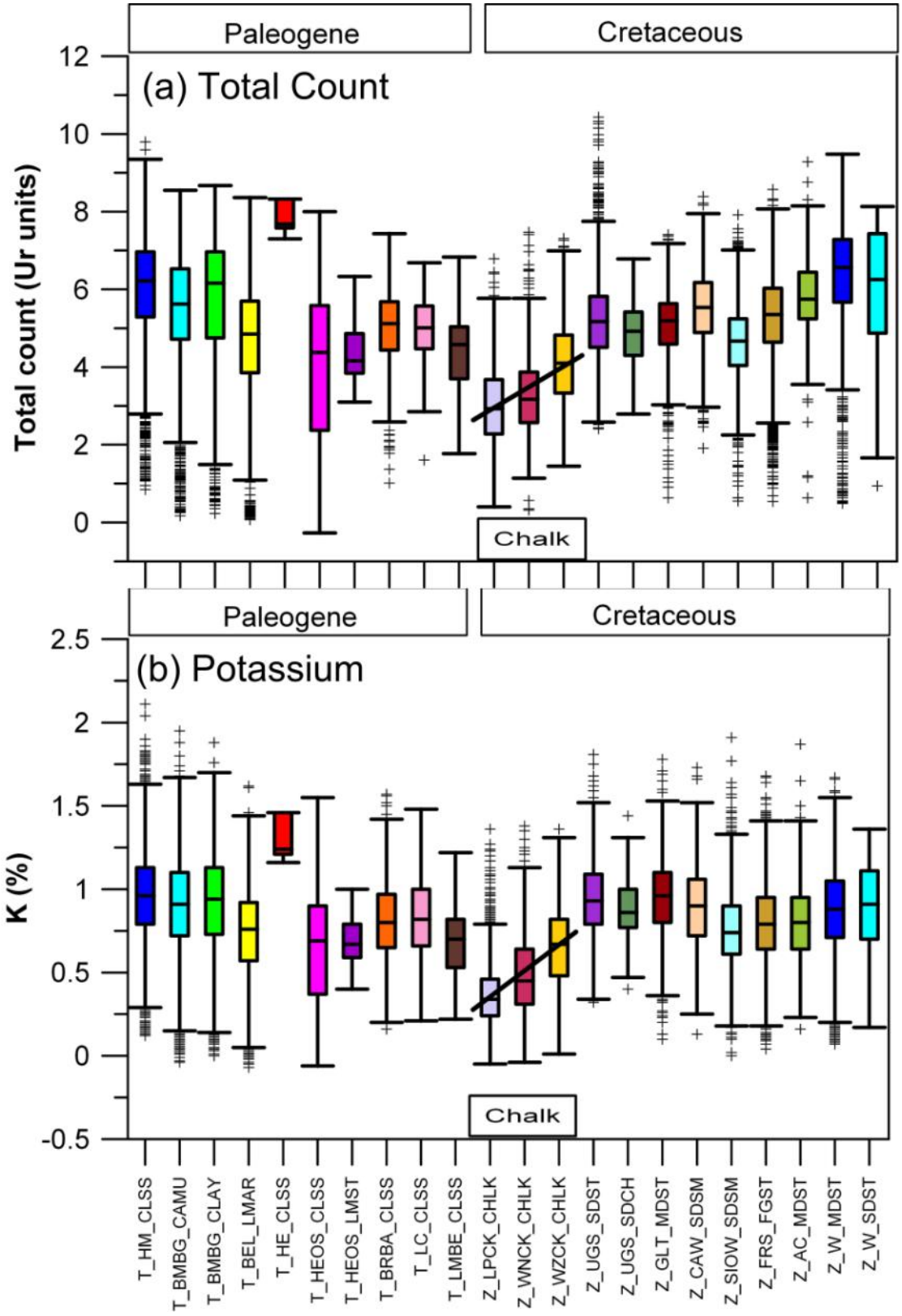
Paleogene
Cretaceous
(a) Total Count
Total count (Ur units)
12
10
8
6
4
2
0
Chalk
Paleogene
Cretaceous
(b) Potassium
K (%)
2.5
2
1.5
1
0.5
0
-0.5
Chalk
T_HM_CLSS
T_BMBG_CAMU
T_BMBG_CLAY
T_BEL_LMAR
T_HE_CLSS
T_HEOS_CLSS
T_HEOS_LMST
T_BRBA_CLSS
T_LC_CLSS
T_LMBE_CLSS
Z_LPCK_CHLK
Z_WNCK_CHLK
Z_WZCK_CHLK
Z_UGS_SDST
Z_UGS_SDCH
Z_GLT_MDST
Z_CAW_SDSM
Z_SIOW_SDSM
Z_FRS_FGST
Z_AC_MDST
Z_W_MDST
Z_W_SDST

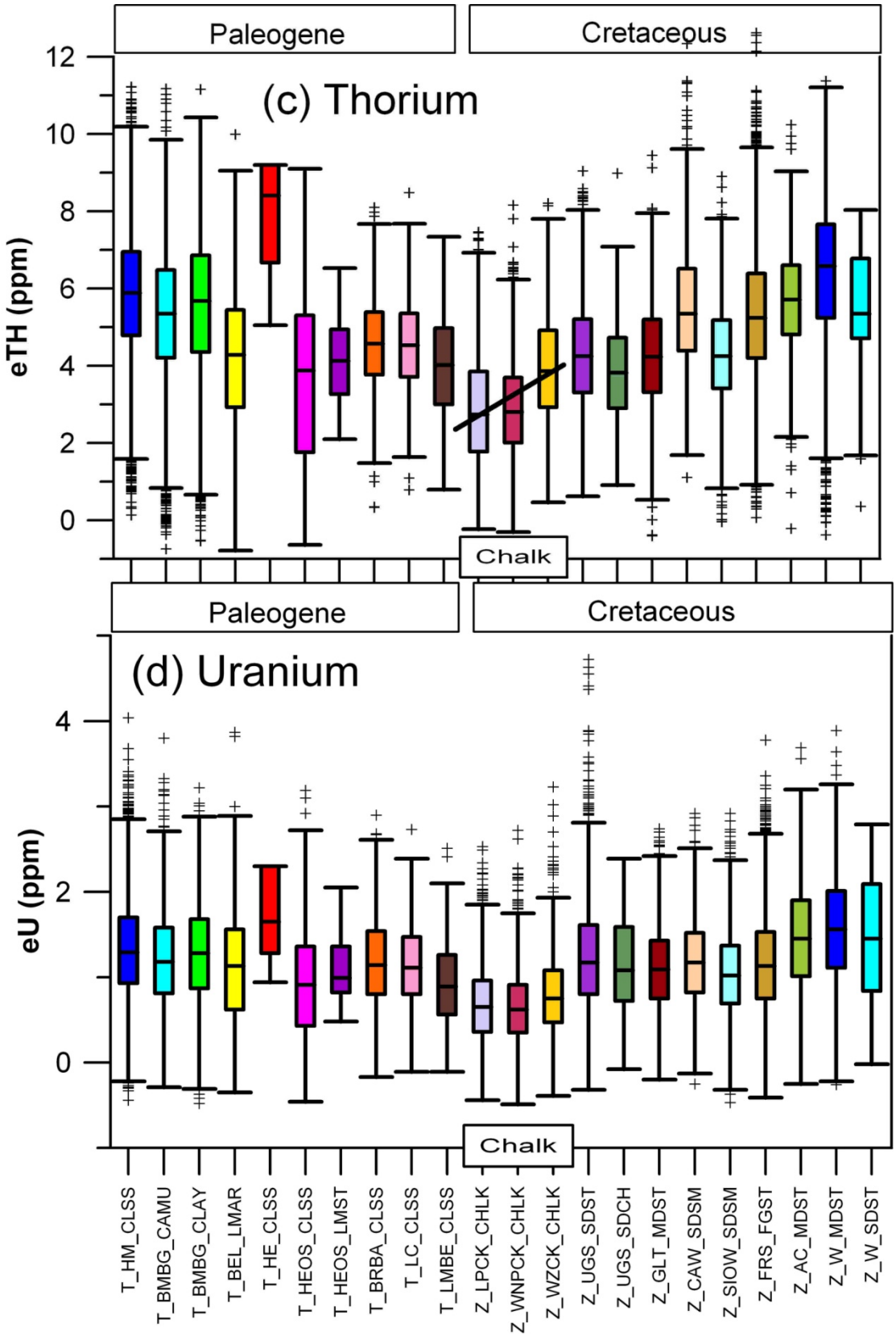
Paleogene
Cretaceous
(c) Thorium
eTH (ppm)
12
10
8
6
4
2
0
Chalk
Paleogene
Cretaceous
(d) Uranium
eU (ppm)
4
2
0
Chalk
T_HM_CLSS
T_BMBG_CAMU
T_BMBG_CLAY
T_BEL_LMAR
T_HE_CLSS
T_HEOS_CLSS
T_HEOS_LMST
T_BRBA_CLSS
T_LC_CLSS
T_LMBE_CLSS
Z_LPCK_CHLK
Z_WNPCK_CHLK
Z_WZCK_CHLK
Z_UGS_SDST
Z_UGS_SDCH
Z_GLT_MDST
Z_CAW_SDSM
Z_SIOW_SDSM
Z_FRS_FGST
Z_AC_MDST
Z_W_MDST
Z_W_SDST

Figure 4

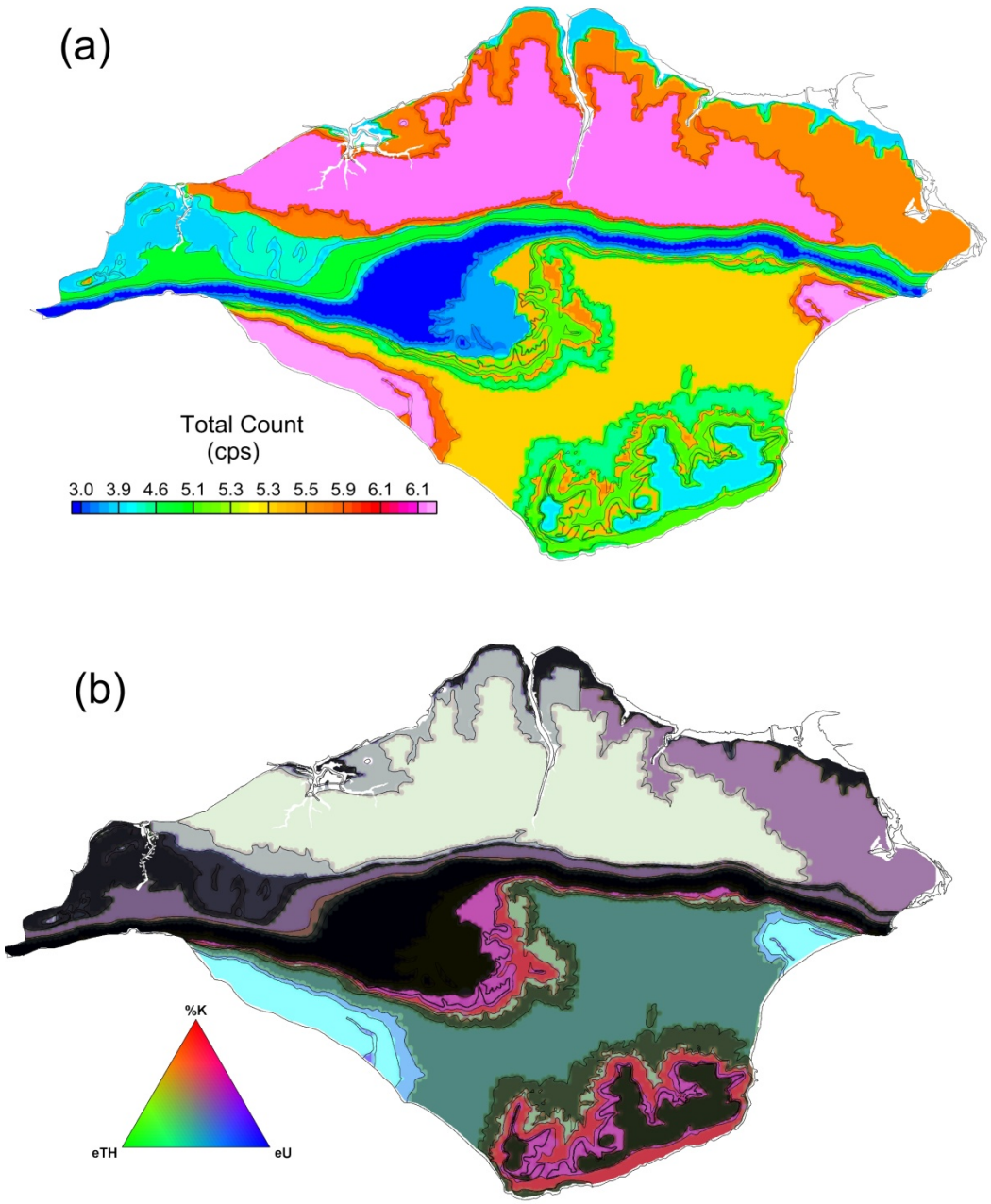

Figure 5

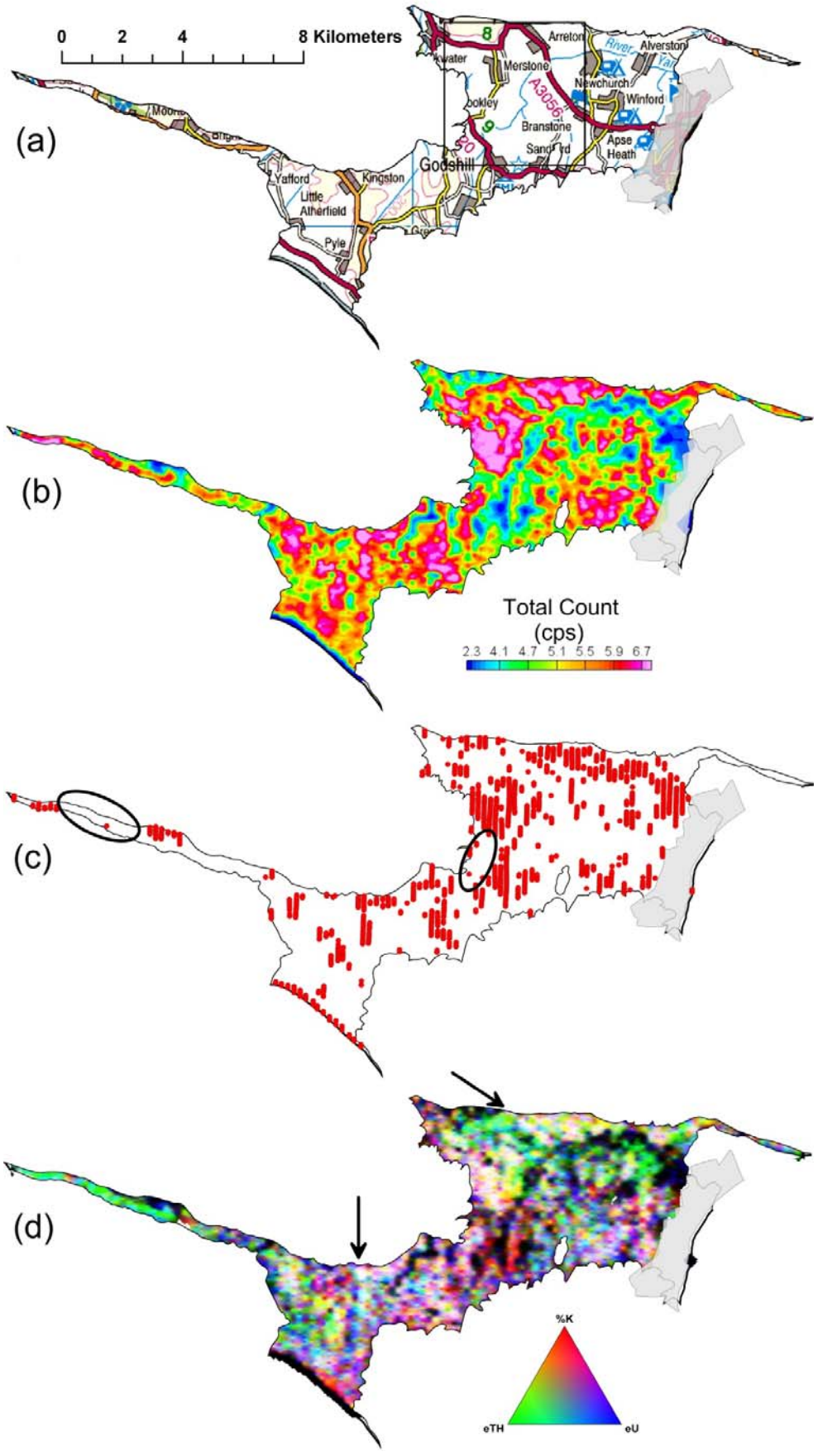
0 2 4 8 Kilometers
(a)
Arreton
Alverston
Merstone
Newchurch
Winford
Branstone
Apse Heath
Goodshill
Yafford
Kingston
Little Atherfield
Pyle
A3056
(b)
Total Count
(cps)
2.3 4.1 4.7 5.1 5.5 5.9 6.7
(c)
(d)
%K
eTH
eU

Figure 6

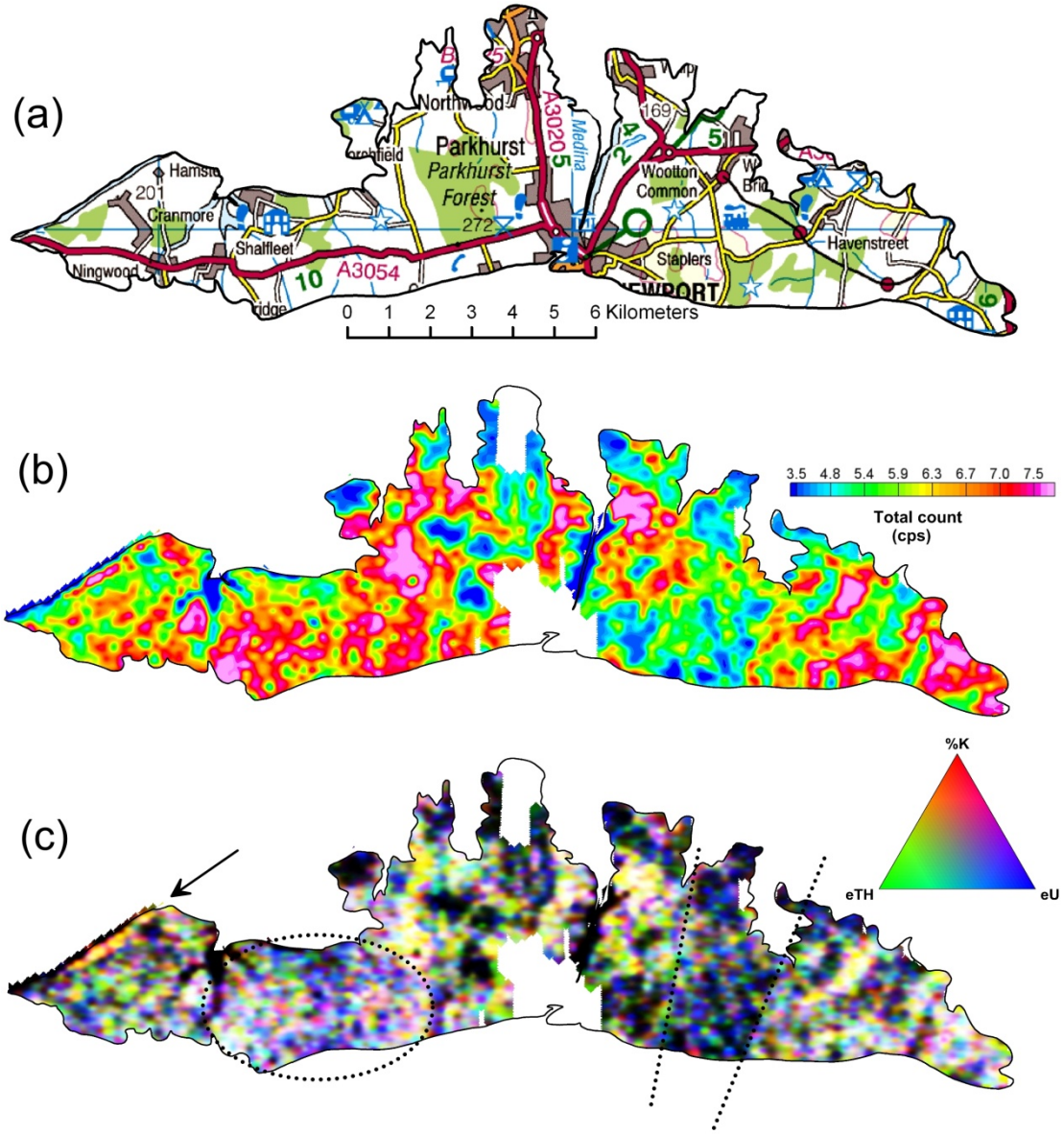
(a)
Parkhurst
Parkhurst Forest
Wootton Common
Staplers
Havenstreet
Shalfleet
Cranmore
Ningwood
A3054
A3020
Medina
0 1 2 3 4 5 6 Kilometers
(b)
3.5 4.8 5.4 5.9 6.3 6.7 7.0 7.5
Total count (cps)
(c)
%K
eTH
eU

Figure 7

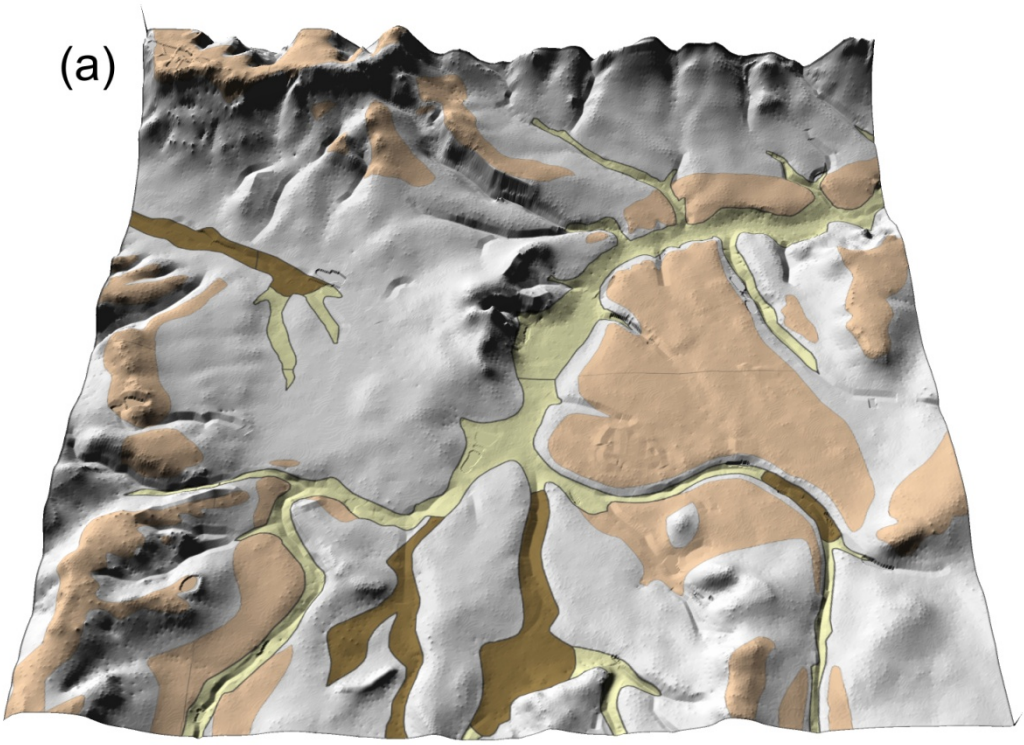
(a)

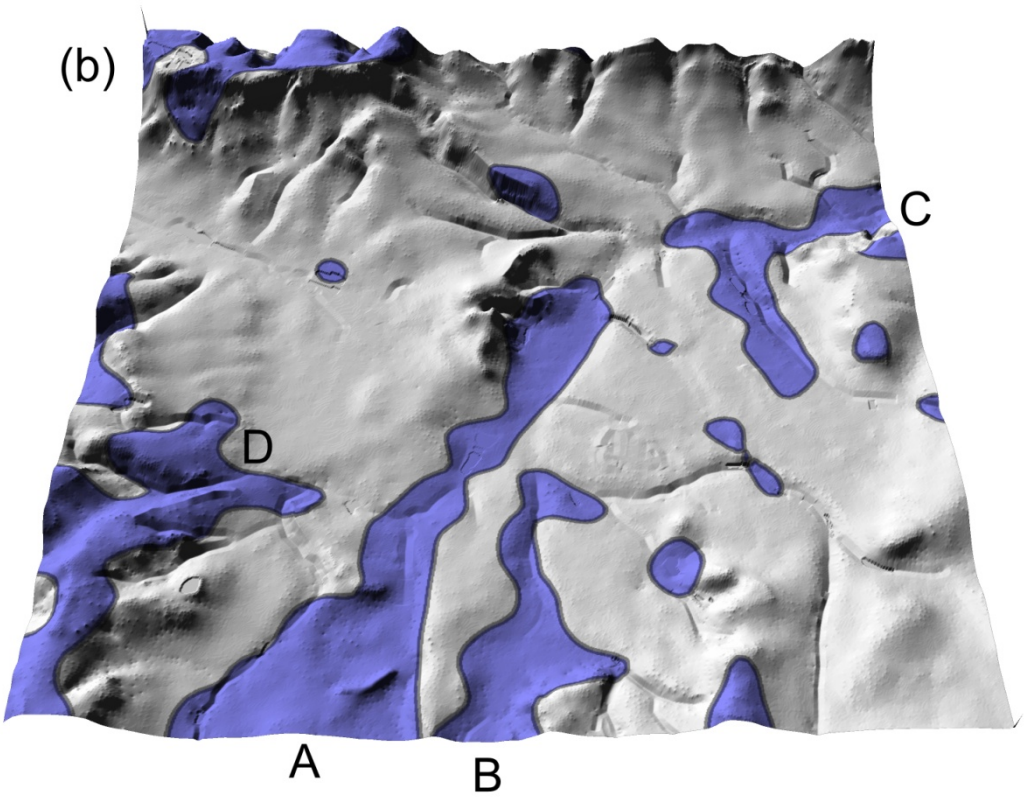
(b)
C
D
A
B

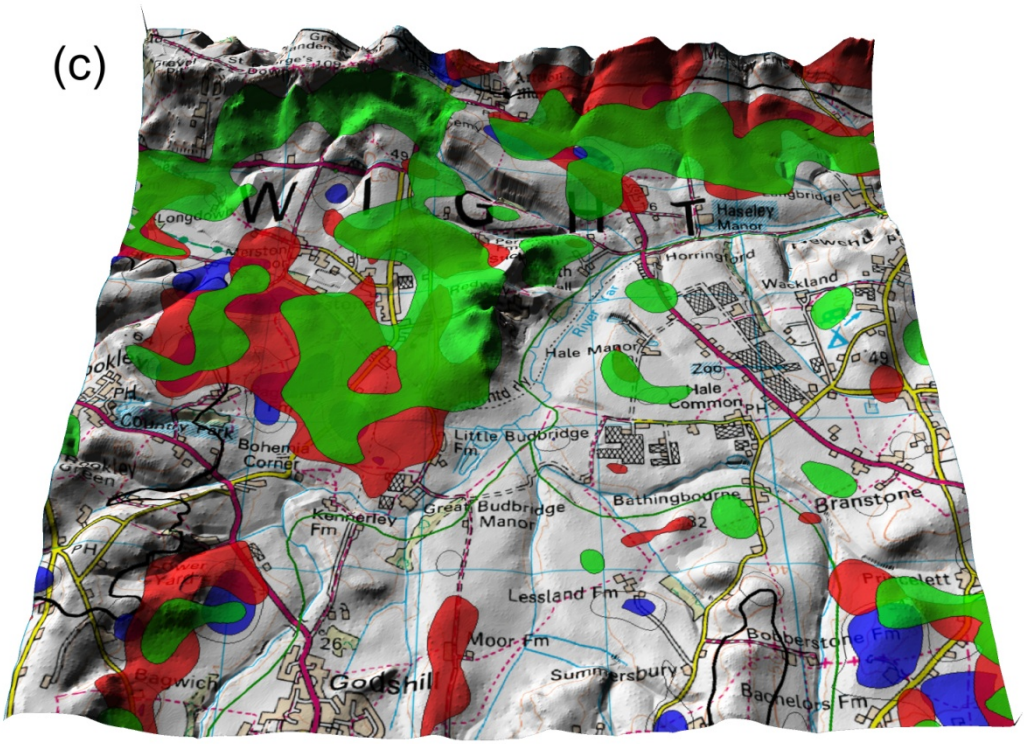
(c)
W I G H T
Haseley Manor
Horringford
Wackland
Hale Manor
Zoo
Hale Common
Little Budbridge Fm
Great Budbridge Manor
Bathingbourne
Branstone
Kennerley Fm
Lessland Fm
Moor Fm
Godshill
Summersbury
Bottberstone Fm
Bachelors Fm
Bohemia Corner

Figure 8